Mineralogical Magazine, June 2018, Vol. 82(3), pp. 577–592

Inclusions in an isoferroplatinum nugget from the Freetown Layered Complex, Sierra Leone

JOHN F. W. BOWLES[1,*], SAIOA SUÁREZ[2,3], HAZEL M. PRICHARD[2,†] AND PETER C. FISHER[2]

[1] School of Earth and Environmental Sciences, University of Manchester, Manchester M13 9PL, UK
[2] School of Earth and Ocean Sciences, Main College. Park Place, Cardiff University, Cardiff, Wales CF10 3AT, UK
[3] Department of Mineralogy and Petrology, UPV/EHU, 48940 Leioa and Ikerbasque, 48011 Bilbao, Spain

[*Received 22 August 2017; Accepted 11 March 2018; Associate Editor: Iain McDonald*]

ABSTRACT

Inclusions of platinum-group minerals (PGM) within alluvial isoferroplatinum nuggets from the Freetown Peninsula, Sierra Leone, are aligned with their shape determined by the structure of their host. The edges of the majority of the inclusions lie at 0°, 45° or 90° to external crystal edges of the nugget which shows that the inclusions are not randomly oriented earlier minerals incorporated within their host. The inclusions are later infills, probably formed at the surface of the nugget during growth and subsequently enclosed by the growing nugget. PGM on the present surface of the nugget represent the last stage of this partnership. A single nugget containing abundant inclusions is described here but similar features are observed in other nuggets from the same area. The inclusions contain laurite (RuS_2), irarsite–hollingworthite (IrAsS–RhAsS), Pd–Te–Bi–Sb phases, Ir-alloy, Os-alloy, Pd-bearing Au, an Rh–Te phase, Pd–Au alloy and Pd–Pt–Cu alloy. PGM found on the nugget surface include laurite, irarsite and cuprorhodsite ($CuRh_2S_4$). The Pd–Te–Bi–Sb phases may include Sb-rich keithconnite ($Pd_{20}S_7$) and compositions close to the kotulskite–sobolevskite solid-solution series (PdTe–BiTe). Textural evidence suggests that formation of the nuggets began with the isoferroplatinum host and the voids were filled starting intergrowths of laurite and irarsite–hollingworthite with both laurite and irarsite–hollingworthite often showing compositional zonation and each of them replacing the other. Filling of the voids probably continued with Pd-Cu-bearing gold, Sb-rich keithconnite $(Pd,Pt)_{20.06}(Te,Sb,Bi)_{6.94}$, keithconnite, telluropalladinite $Pd_9(Te,Bi)_4$, RhTe and finally Ir-alloy and then Os-alloy. The nuggets are thought to be neoform growths in the organic- and bacterial-rich soils of the tropical rain forest cover of the Freetown intrusion. The mineralogical assemblage in the layered gabbros of the intrusion has been previously shown to differ from the alluvial assemblage in the rivers and these inclusions, not seen in Pt_3Fe in the unaltered rocks, add a further item to the catalogue of differences.

KEYWORDS: platinum-group minerals, Freetown Intrusion, Sierra Leone, alluvial, inclusions, neoform.

Background

INVESTIGATION of the alluvial platinum-group minerals (PGM) of the Freetown Intrusion, Sierra Leone included panning of gravel from rivers recorded as PGM-bearing (Bowles *et al.,* 2018). Rivers mentioned in the older literature (Pollett, 1931, 1951) were panned, accompanied by pitting and panning in the adjacent river terraces of the largest river, the Big Water, near York in the centre of the Freetown Peninsula (Fig. 1). The PGM recovered were 0.1 to 1.5 mm in size and include Cu-bearing isoferroplatinum (Pt_3Fe) and disordered $Pt_{3-x}Fe$, ($x \leq 0.38$), tulameenite (Pt_2FeCu), hongshiite (PtCu), cooperite–vysotskite (PtS–PdS), laurite (RuS_2), erlichmanite (OsS_2), Os–Ir

*E-mail: john.bowles@manchester.ac.uk
†Deceased Jan 2017
https://doi.org/10.1180/mgm.2018.85

This paper is published as part of a thematic set in memory of Professor Hazel M. Prichar

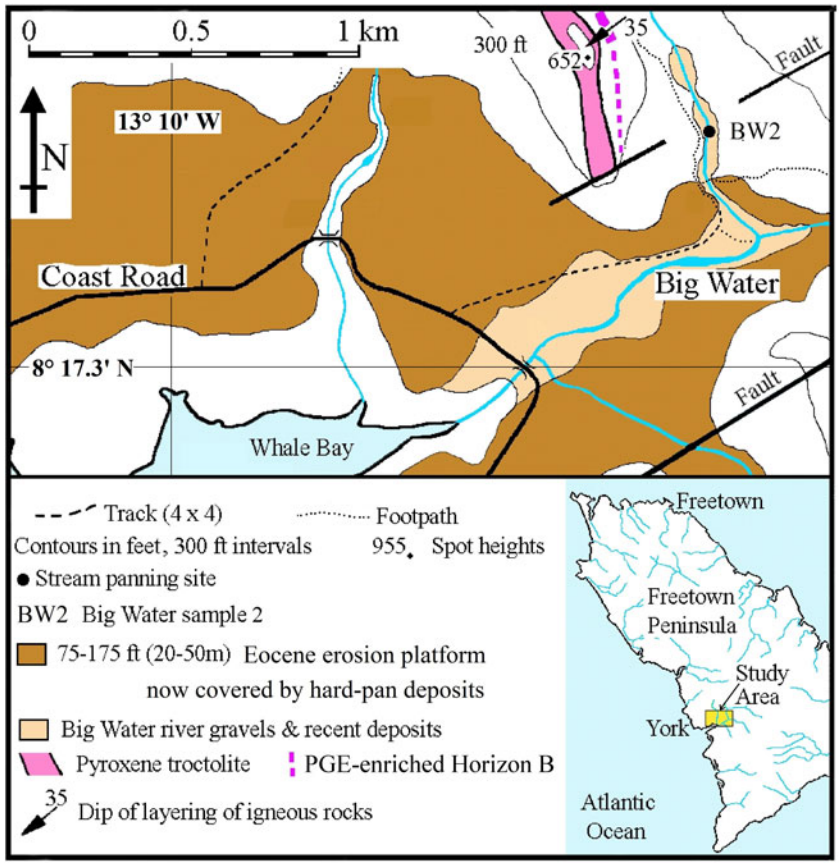

FIG. 1. Map of part of the Freetown Peninsula showing the BW2 sampling site.

alloy, Os–Ru alloy and native copper (Bowles *et al.,* 2018). One sample site (BW2) in the Big Water river yielded a black sand that assayed 14.90 g/t Pt, 0.18 g/t Pd and 0.03 g/t Au. Platinum greatly in excess of Pd and Au is typical of all of the samples from the area. Further panning and hand-picking of the sample from BW2 located 11 isoferroplatinum (Pt_3Fe) nuggets and two nuggets of disordered $Pt_{3-x}Fe$ (with $x = 0.19–0.27$). The nuggets measure 0.1 to 0.6 mm across (Bowles *et al.* 2018). Whilst several of the nuggets contain inclusions of other PGM, one example (nugget BW2-12) contains many inclusions of laurite, irarsite–hollingworthite, Pd–Te±Sb±Bi phases, Ir and Os alloys with variable Ru, Pt and Rh contents and Au–Pd–Cu alloy. This nugget is examined in detail here.

It has been suggested that the contrast between the mineral assemblage, mineral chemistry and grain size of the PGM in the known primary occurrences of the Freetown Intrusion and the alluvial assemblage could best be explained by growth of neoform nuggets in the soil (Bowles, 1986). Recent evidence supports this view (Bowles *et al*., 2017, 2018) although not everybody has been convinced by this proposal (e.g. Hattori *et al*., 1991). Bowles *et al*. (2013, 2017) show the complete sequence of alteration of the PGM from the fresh rocks in the main platinum-group element (PGE)-enriched layer known in the complex (Bowles, 2000*a*) to the weathered rocks and to the saprolite formed under tropical weathering conditions. The weathering process is marked by initial oxidation of PGE-bearing sulfides and PGM followed by modification of the mineral assemblages and selective leaching of Pt, Pd and Au which enter the saprolite and are leached down slope from the mineralized horizons. Progressive

https://doi.org/10.1180/mgm.2018.85 Published online by Cambridge University Press

destruction of the PGM and metal leaching as weathering proceeds provide PGE for the later re-precipitation of eluvial and alluvial PGM in soils close to the rivers or stream banks due to changes in the geochemistry or biogeochemistry of the PGE-solutions. The contrasting mineralogy and textural features of the alluvial PGM compared to the PGM assemblage in the source rocks are detailed in Bowles *et al*. (2018). The high rainfall, thick cover of vegetation and long period of weathering (erosion of the 20–50 m platform now covered by the hard pan shown in Fig. 1 dates from the Eocene) have allowed organic compounds to contribute to weathering, transport and deposition of the PGE (Bowles *et al*., 1995, 2018). The growth of nuggets may have been bacterially aided (Reith *et al*., 2016; Campbell *et al*., 2018). The significance of the inclusions is that they are not earlier than the nuggets as suggested by Hattori *et al*. (1991) who saw them as entrained by their host in an early magmatic setting or possibly exsolution products. It is argued here that such inclusions post-date their host.

Methods

The alluvial samples consisted of black sand concentrates panned from the Big Water river bed by a team of local workers. The concentrate was split using a riffle splitter and a split assayed for Pt, Pd and Au by Lakefield Research in Canada. Another split was panned again in the laboratory to recover the densest fraction and the PGM nuggets found during the process were hand picked; nugget BW2-12 was found at this stage. All the PGM recovered from the samples were mounted separately on stubs for examination of their morphology and, subsequently, in polished blocks for analysis using scanning electron microscopy. This study used a Cambridge Instruments ZEISS NTS S360 scanning electron microscope (SEM) coupled to an Oxford Instruments INCA Energy system with an energy dispersive X-ray analytical system (EDX) at Cardiff University (UK). A set of pure element standards were used to calibrate the EDX system. Qualitative analyses were carried out for all of the inclusions in nugget BW2-12 and quantitative analyses were possible for the larger (2–12.5 μm) inclusions. Operating conditions for the quantitative analyses were 20 kV, with a specimen current of 1 nA, and a working distance of 10 mm. Counting livetime was 50 s, and a cobalt reference standard was measured every 20 min to compensate for beam drift. Repeat analyses were performed to check for homogeneity and consistency. Analysing minute multi-mineral inclusions using SEM plus EDX requires great care and we document the steps taken to achieve this below. A finely focussed (1 nA) electron beam was used. This presents two main difficulties for analysis. Firstly the beam current is low so the X-ray count rate is reduced with an adverse effect on the counting statistics and the resultant analytical precision. Secondly, the detailed images available from the back-scattered electrons (BSE) do not represent the lower resolution, analysed volume below the sample surface. The latter problem is significant if the analysed volume includes minerals that are not evident at the surface or are a part of the host mineral. In an effort to overcome these difficulties the inclusions have been analysed during five sessions with multiple analyses of each inclusion in slightly different positions. The section was repolished between analytical sessions 2 and 3 to present a slightly different surface and volume for analysis and highlight those analyses that varied with depth. The fine-scale (sub-micrometre) zonation of some of the laurite and the irarsite–hollingworthite cannot be fully differentiated by the analyses. The points chosen for analysis of zoned minerals were those where the zonation is coarsest, but the analyses cannot represent the complete range of the zonation. Only consistent and reproducible analyses have been used leaving 427 analyses considered suitable. In analyses where both Fe and Pt are present, 98 of these analyses with Pt/Fe in a similar ratio to Pt_3Fe have also been discarded under the assumption that the analysed volume contains some of the isoferroplatinum host below the surface. These discarded analyses are from inclusions measuring less than 2 μm × 2 μm in size and some up to 3 μm in one dimension. It appears that the method is capable of analysing inclusions above 2 μm × 2 μm in size. The discarded analyses of the slightly larger inclusions are those where analysis of a different part of the inclusion does not contain Pt and Fe so these discarded analyses are presumed to be due to the presence of Pt_3Fe at depth. The remaining 329 analyses are not perfect but represent a reasonable first description of the inclusions and encourage the belief that the analyses offer an adequate measure of the composition (Table 1). More details of the alluvial sampling and analyses are to be found in Bowles *et al*. (2018).

https://doi.org/10.1180/mgm.2018.85 Published online by Cambridge University Press

TABLE 1. A polished section of nugget BW2-12 contains 98 inclusions composed of 190 PGM+Au phases.

Type of PGM	No. of included minerals	Area of inclusion (μm^2)	%		Size (μm)		No. of inclusions analysed	Number of inclusions analysed, arranged by size (μm)								No. of analyses made	No. of accepted analyses
			No. of minerals	Area	Min	Max		0.1[a] 0.5–1[b]	1[a] 1–2[b]	2[a] 2–3[b]	3[a] 3–8[b]	4[a] 5–9[b]	5[a] 5–7[b]	6[a] 7–8[b]	4[a] 8–13[b]		
Laurite	27	308.1	14.2	24.5	0.5	12.5	24		1	7	9	2			5	92	54
Irarsite–hollingworthite	21	160.7	11.1	12.8	0.3	9.0	13	1	1	6	1	3			1	53	44
PGE-tellurides:																	
(i) Pd–Sb–Te	7	103.4	3.7	8.2	1.7	6.5	7			1	2		4			24	24
(ii) Pd–Te–Sb–Bi	27	277.7	14.2	22.1	0.1	8.0	26		4	7	8	2	3	2		71	56
(iii) Pd–Te–Bi–Sb	34	170.9	17.9	13.6	0.4	7.0	23	1	1	10	8	1	1	1		48	31
(iv) Pd–Te–Bi	8	44.6	4.2	3.5	0.5	4.4	8	1	1	4	2					24	19
(v) Rh–Te ± (Pd–Bi)	3	6.2	1.6	0.5	1.1	2.7	3		1	2						11	11
Iridium	34	94.2	17.9	7.5	0.2	4.0	27	5	13	7	2					50	42
Gold (Au–Pd–Cu)	21	89.7	11.1	7.1	0.1	7.0	19	4	4	6	5					33	29
Osmium	5	0.6	2.6	0.1	0.08	1.57	5	5								9	7
Cooperite	1	0.5	0.5	0.04	0.50	2.00	1		1							3	3
Pd–Pt–Cu	1	0.5	0.5	0.04	0.34	3.13	1			1						7	7
Pd–Au	1	0.3	0.5	0.02	0.10	0.30	1	1								2	2
Total	190	1257	100.0	100.0	0.1	12.5	158	18	27	51	37	8	8	3	6	427	329
Nugget section		59,373			191	410		analyses discarded		some analyses accepted	analyses accepted						
Area of inclusions as % nugget area				2.1													

Results

Nugget BW2-12, Big Water river

This nugget consists of ordered isoferroplatinum (Pt_3Fe) with an average composition of $(Pt_{2.86}Rh_{0.01}Pd_{0.07}Ru_{0.01})_{2.95}(Fe_{1.02}Cu_{0.04})_{1.06}$. In part the nugget has an irregular shape, but crystal faces can be distinguished (Fig. 2). It is 190 μm × 410 μm in size, and it has large PGM up to 30 μm in size attached to its surface (Fig. 2*a*). These PGM are laurite [$(Ru,Rh)S_2$], irarsite [(Ir,Rh)AsS] and cuprorhodsite [$(Cu,Fe)(Rh,Pt,Ir)_2S_4$].

A polished section of this nugget (Fig. 2*b*) contains 98 small inclusions of PGE- and Au-bearing minerals that are between 2 and 12.5 μm across. They occupy 2.1% of the surface area of the section. Most (72%) are composite inclusions containing 2–4 different minerals; the remaining inclusions (28%) are monomineralic (Table 1). The majority of the inclusions have sharp, well-defined boundaries and only a few (4%) show anhedral to subrounded or diffuse boundaries.

The shape of the inclusions

Many of the larger inclusions show one or more straight edges in the polished section which must represent planes in three dimensions. Measurements of the angles between 266 of these linear edges from 42 inclusions, using an external crystal face of the nugget as a reference, show that the edges group predominantly into specific directions (Fig. 3). The dominant angles are 0–8°, 44.8°, 92.7°, 132° that approximate to the angles (0°, 45°, 90°, 135°) between the (100) and (111) faces of the cubic host. These inclusion edges are clearly determined by the cubic structure of the host nugget. They show that the area covered by the measurements represents a single crystal and that the inclusions began as voids shaped by internal crystal faces of the host. Other nuggets from the Freetown Peninsula do not contain so many inclusions but they show the same control of the inclusion shape. Measurements of the angles of the inclusion edges for three such nuggets are shown by the insets to Fig. 3.

Many inclusions (41%) are composed of Pd-rich PGM of the Pd–Te–Bi–Sb system. These are Pd-rich tellurides with variable contents of Bi and Sb (Table 1, Figs 2 and 4). The next most abundant PGM are laurite and members of the irarsite–hollingworthite solid-solution series (25% abundance), which usually occur in composite inclusions. Less abundant PGM are iridium (18%), gold (11%) and Os-alloys (3%) that are commonly associated with the Pd-rich inclusions. In addition, two grains of Pd–alloys (Pd–Pt–Cu and Pd–Au) and a grain of cooperite (PtS) are present in the nugget (totalling 2%). Similar inclusions occur in other nuggets from the same area and the nugget described here differs only in the large number of inclusions it contains. The different types of inclusion seem to be scattered across the section and not grouped by size or mineral association. The compositions of the host, the inclusions and the minerals attached to the nugget surface are shown in Table 2.

Composition of the inclusions

Laurite and irarsite–hollingworthite

Laurite is present in 27 large inclusions up to 10 μm × 12.5 μm across (5.5 μm on average), all with well defined outlines. Most (81%) of these inclusions are composite and contain both laurite and members of the irarsite–hollingworthite series. These phases show varied mutual intergrowth or replacement textures often with strong zonation parallel to the walls of the inclusion or irregular zonation (Fig. 5*a*–*e*). In four cases laurite occurs with Pd-tellurides forming inclusions that also contain Ir or Au and PtS (Fig. 5*e*), and in one case it is seen as a single zoned crystal 5 μm across. The textural relationships between laurite and irarsite allow two groups of inclusions to be distinguished: (1) Laurite cut by later sulfarsenides; and (2) Laurite replacing sulfarsenides; these account for 57% of the laurite–irarsite inclusions. These inclusions show that laurite and irarsite can be intergrown and that several generations of laurite and irarsite–hollingworthite may be present. Some 54 analyses show that laurite contains minor proportions of Ir (6–16%) and Rh (0–7%). Palladium and Os are generally absent but 1% Os is seen in two analyses. Platinum (2–14%) is also present in 25 analyses, generally in the centre of zoned laurites. This Pt is not accompanied by detectable Fe so it does not indicate interference in the analyses from the Pt_3Fe hosting the inclusions. Arsenic (1–7%) occurs in some analyses but it does not correlate 1:1 with Ir so the Ir and As appear to be constituents of the laurite rather than interference in the analyses from the associated irarsite–hollingworthite. Analyses of laurite and irarsite are shown in Table 2.

https://doi.org/10.1180/mgm.2018.85 Published online by Cambridge University Press

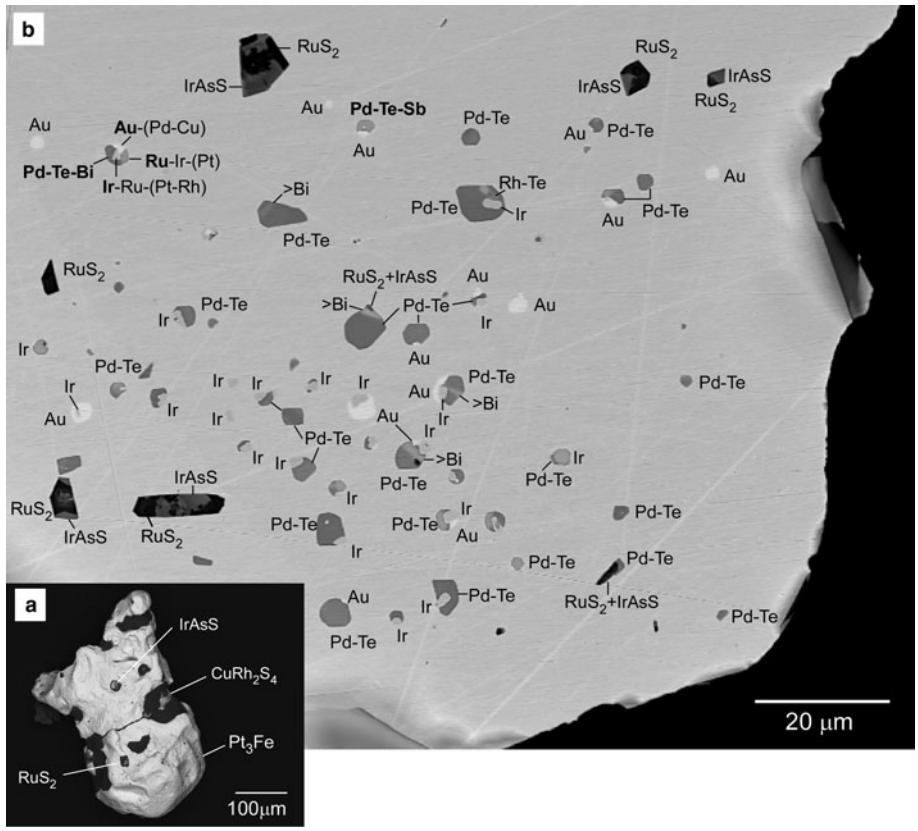

FIG. 2. Nugget BW2-12 showing (*a*) the complete nugget and (*b*) a polished section containing many PGE+Au inclusions.

Laurite replacing irarsite and hollingworthite

This laurite is typically not zoned and it replaces irarsite–hollingworthite (Fig. 5*a–b*). In Fig. 5*a* the irarsite–hollingworthite occurs in two parts, each part with a zonation that follows the same pattern. The laurite cuts across this pattern and is clearly later than the irarsite–hollingworthite. These textures are emphasized in the insets to Fig. 5*a*. Locally the Pt content can reach up to 13 wt.% which produces diffuse, Pt-rich areas within the inclusions (Fig. 5*b*). The sulfarsenides are sometimes zoned, varying in composition from irarsite to hollingworthite and the zonation can be parallel to the wall of the inclusion or the zonation can be irregular. Replacement by unzoned laurite cuts the zonation of the irarsite–hollingworthite and leaves cuspate edges (Fig. 5*a*). In several inclusions the sulfarsenides are unzoned and typically remain as relict grains along the internal walls of the inclusion (Fig. 5*b*).

Laurite replaced by irarsite–hollingworthite

This laurite is very often zoned (Fig. 5*c–d*). The inclusions show a common pattern with a strongly zoned laurite in the core forming layers parallel to the walls that are followed by layers of a mixed composition with high Ir, Rh and As contents, and followed outwards by unzoned laurite. One inclusion (Fig. 5*d*) has a central zoned laurite surrounded by well-developed layers of hollingworthite [(Rh, Ir,Ru)AsS] continuing the zoning which lead into an unzoned grain of irarsite [(Ir,Rh,Ru)AsS] with irregular margins. Irarsite is then followed by unzoned laurite. These textures are emphasized in the inset to Fig. 5*d*.

Pd-tellurides with antimony and bismuth

In nugget BW2-12 a total of 65 of the 98 inclusions contain one or more examples from the Pd–Te–Bi–Sb system. Most contain minor

https://doi.org/10.1180/mgm.2018.85 Published online by Cambridge University Press

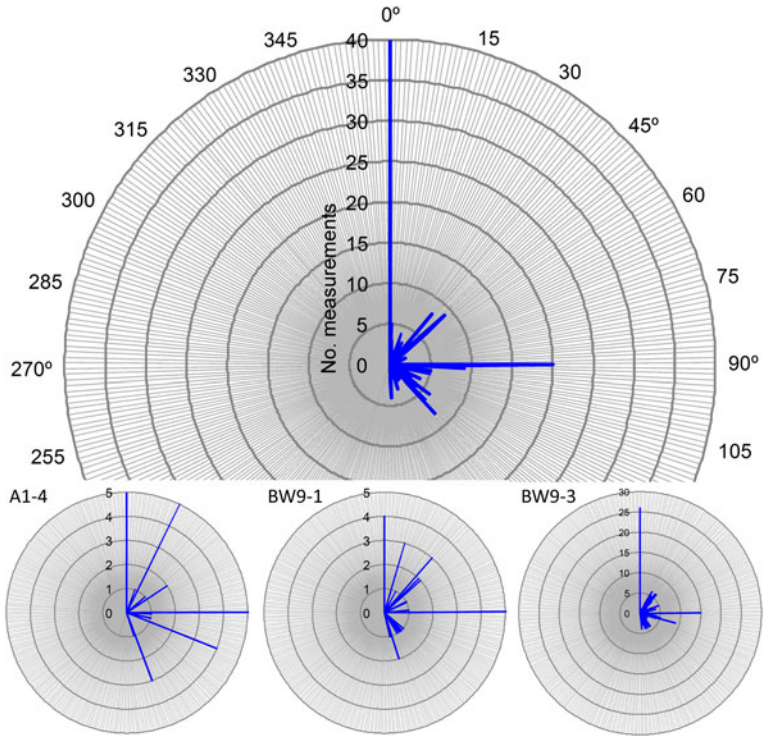

FIG. 3. The directions of inclusion edges (BW2-12) relative to an external crystal face. The insets show similar measurements for other nuggets.

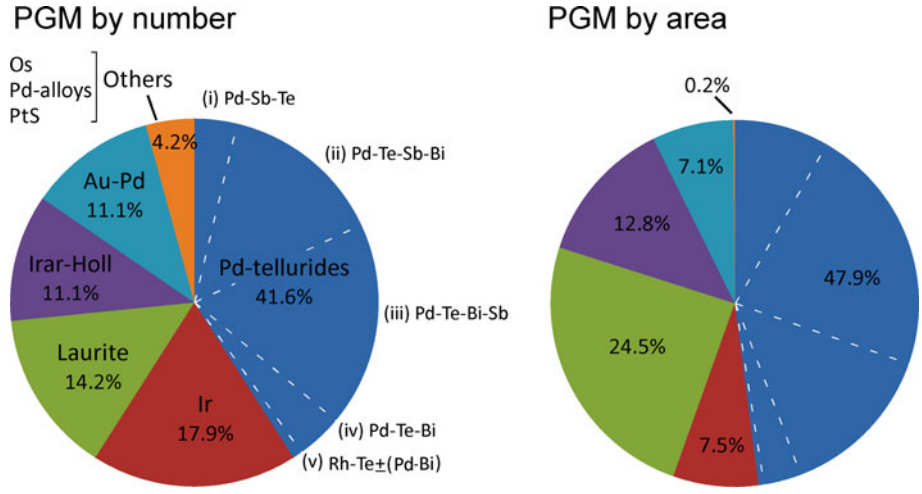

FIG. 4. Proportions of the PGM+Au phases forming the inclusions.

amounts of Pt, a few have a significant Rh content and others contain a little Ru or Ir. Their composition is notable for a variation in the Bi and Sb content. This variation is arguably continuous but there appear to be clusters in composition which make it possible to distinguish

https://doi.org/10.1180/mgm.2018.85 Published online by Cambridge University Press

TABLE 2. Compositions of the host nugget, the inclusions and the external PGM.

Analysis No.	1 BW2-12 Fig. 5 host	2 Laurite Fig. 5a	3 Irar-holl Fig. 5a	4 $Pd_{20}(Sb,Te)_7$	5 $(Pd)_{20}(Te,Sb)_7$	6 $Pd_9(Te,Bi)_4$	7 $Pd_3(Bi,Te)_2$	8 $?Pd_5(Te,Bi)_4$	9 $Au_{0.7}Pd_{0.2}Cu_{0.1}$	10 Laurite	11 Irarsite	12 Cupro-rhodsite
Pt	88.95	1.81	2.83	2.41	1.26	6.2	10.08	8.24	1.44	–	–	27.63
Rh	0.14	6.66	25.34	–	–	–	–	–	–	2.11	11.26	16.40
Pd	1.21	–	–	69.92	69.80	56.42	42.64	38.2	9.06	–	–	–
Ir	–	12.45	26.82	–	–	–	–	–	–	–	47.67	18.90
Ru	–	40.06	3.40	–	–	–	–	–	–	58.63	–	–
Fe	9.12	–	–	–	–	–	–	–	–	–	–	0.86
Cu	0.41	–	–	–	–	–	–	–	3.86	–	–	13.13
As	–	6.98	25.87	–	–	–	–	–	–	–	26.76	–
Sb	–	–	–	15.61	6.41	–	–	–	–	–	–	–
Te	–	–	–	11.10	22.53	26.79	24.43	24.39	–	–	–	–
Pb	–	–	–	–	–	–	–	–	–	3.92	–	–
Bi	–	–	–	0.71	–	10.59	22.85	29.08	–	–	–	–
Au	–	–	–	–	–	–	–	–	82.89	–	–	–
Hg	–	–	–	–	–	–	–	–	2.47	–	–	–
S	–	31.55	15.81	–	–	–	–	–	–	35.35	14.31	23.08 23.08
Total	99.83	99.51	100.07	99.75	100.00	100.00	100.00	99.91	99.72	100.01	100.00	100.00
Pt	2.86	0.02	0.03	0.38	0.20	0.50	0.34	0.52	0.01	–	–	0.74
Rh	0.01	0.12	0.58	–	–	–	–	–	–	0.04	0.28	0.83
Pd	0.07	–	–	19.98	19.86	8.38	2.66	4.42	0.15	–	–	–
Ir	–	0.12	0.33	–	–	–	–	–	–	–	0.64	0.51
Ru	–	0.74	0.08	–	–	–	–	–	–	1.02	–	–
Fe	1.02	–	–	–	–	–	–	–	–	–	–	0.08
Cu	0.04	–	–	–	–	–	–	–	0.10	–	–	1.07
As	–	0.17	0.81	–	–	–	–	–	–	–	0.92	–
Sb	–	–	–	3.90	1.59	–	–	–	–	–	–	–
Te	–	–	–	2.65	5.35	3.32	1.27	2.35	–	–	–	–
Pb	–	–	–	–	–	–	–	–	–	0.03	–	–
Bi	–	–	–	0.10	–	0.80	0.73	1.71	–	–	–	–
Au	–	–	–	–	–	–	–	–	0.72	–	–	–
Hg	–	–	–	–	–	–	–	–	0.02	–	–	–

S	–	1.83	1.16	–	–	–	–	–	1.94	1.15	3.75
As+S+Sb+Te+Bi+Pb	2.00	1.98	–	6.94	4.12	2.00	4.06	–	1.97	2.07	3.75
Ru+Ir+Rh+Pt+Pd	1.00	1.02	–	20.06	8.88	3.00	4.94	0.16	1.06	0.92	2.08

Analysis 1 is the average of 4 analyses of the host nugget.
These analyses show consistent values for Pt, Fe, Cu but there is some variability for Rh (0–0.56 wt.%) and Pd (0.84–1.41 wt.%).
Analysis 3 is from a zone of average composition in the zoned irarsite–hollingworthite of Fig. 5*a*.
Analysis 4 is the average of 24 analyses of inclusions of similar composition.
In the text the formula is shown as $Pd_{1.9.98}(Te,Sb,Pt,Bi)_{7.03}$ with Pt included with Te and Sb rather than Pd.
Analyses 10, 11 and 12 are from minerals external to the nugget and not on the polished section.
Every effort was made to select a smooth surface normal to the electron beam but these analyses should be regarded as qualitative.

five groups: (i) Pd–Sb–Te; (ii) Pd–Te–Sb–Bi; (iii) Pd–Te–Bi–Sb; (iv) Pd–Te–Bi; and (v) Rh–Te ± (Pd–Bi), listed here in order of decreasing Sb and increasing Bi and Rh (Table 1). Analyses of inclusions from these groups are shown in Table 2.

Group (i): Pd–Sb–Te

The Pd–Sb–Te group contains 66–71 wt.% Pd, 12–18 wt.% Sb, 9–13 wt.% Te and 0–3 wt.% Bi on the basis of 24 analyses of six inclusions larger than 3 μm × 3 μm (Table 1). The nugget contains seven separate inclusions and the largest is 5 μm × 6.5 μm. They contain an average 2.4 wt.% Pt and the absence of detectable Fe suggests this is not due to interference from the host. These inclusions are located together at one edge of the nugget, perhaps reflecting a localized factor in the incorporation of Sb, and they occur singly or associated with Os that forms elongate crystals of ~0.1 μm × 1.5 μm and with Au (Fig. 5*m,n*). The analyses of these inclusions lie close to $Pd_{20}Te_7$ to $Pd_{20}Sb_7$ in the solid-solution series of Kim and Chao (1991) suggesting that they are Sb-rich keithconnites.

Group (ii): Pd–Te–Sb–Bi

The Pd–Te–Sb–Bi group contains 61–76 wt.% Pd, 13–23 wt.% Te, 0–12 wt.% Sb and 0–9 wt.% Bi. There are 27 examples in the polished section of nugget BW2-12 and the indicated range of composition is based on 52 analyses of examples 3 μm × 3 μm or larger with some analyses of 2 μm × 2 μm inclusions that do not show evidence of interference from the Pt+Fe present in the host (Table 1). Examples free of Fe contain up to 13 wt.% Pt. The analyses from these inclusions also lie close to the $Pd_{20}Te_7$ to $Pd_{20}Sb_7$ solid-solution series (Table 2, anal. 5) and they appear to be a less Sb-rich keithconnite that also contains some Bi. A formula with $(Pd,Pt)_{20.06}(Te,Sb,Bi)_{6.94}$, can be obtained. The maximum length is 8 μm and they are often associated with smaller Ir and/or Au grains. Some occur as single inclusions (Fig. 5*h,i*), occasionally with diffuse Bi-rich areas (Fig. 5*j,k*) or bands. A few include crystals of laurite–irarsite (Fig. 5*e*). Rarely, they contain laths of osmium [Os–Ir–Ru–(Pt)] in composite grains with Pd–Te–Bi–Sb phases (Fig. 5*l*).

Group (iii): Pd–Te–Bi–Sb

The Pd–Te–Bi–Sb group contains 44–67 wt.% Pd, 21–30 wt.% Te, 2–19 wt.% Bi and 2–3 wt.% Sb.

https://doi.org/10.1180/mgm.2018.85 Published online by Cambridge University Press

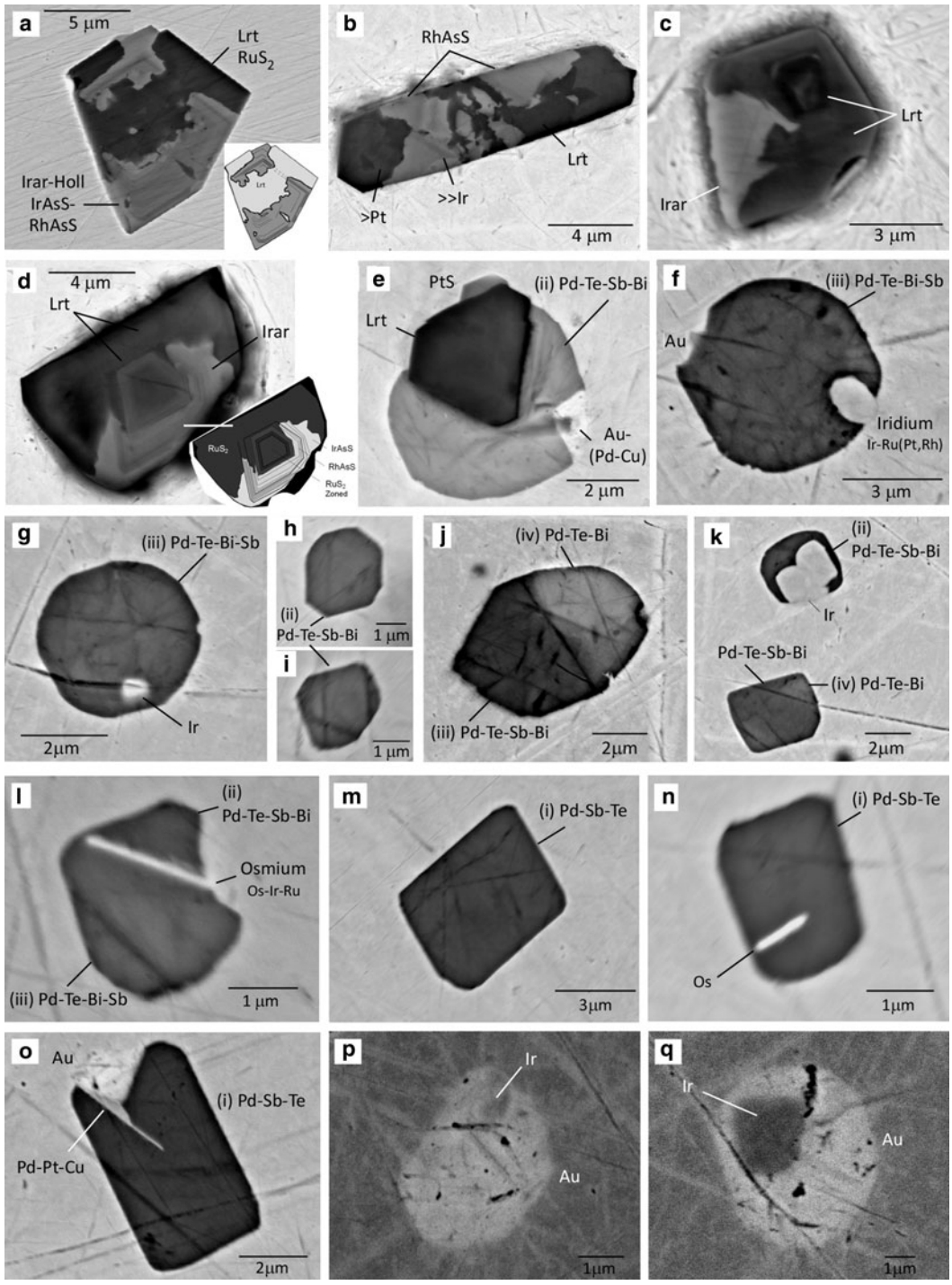

FIG. 5. BSE images of: (*a–d*) large inclusions containing laurite and irarsite–hollingworthite; (*e*) large inclusion of laurite with a Pd–Te PGM and Au; (*f,g,h,i,j,k,l*) inclusions containing Pd–Te (Bi) and Pd–Te (Sb) phases; (*m,n,o*) inclusions containing Pd–Sb phases; and (*p,q*) Au inclusions containing iridium.

https://doi.org/10.1180/mgm.2018.85 Published online by Cambridge University Press

These are more abundant and 34 examples were encountered up to 7 μm across (Table 1). The indicated range of composition is based on 26 analyses of examples 3 μm × 3 μm or larger and analyses of 2 μm × 2 μm inclusions free from interference by Pt+Fe present in the host (Table 1). The analyses cover compositions between the Te-rich part of the $Pd_{20}Te_7$ to $Pd_{20}Sb_7$ solid-solution series and the Pd_8Te_3, Pd_7Te_3, Pd_9Te_4, Pd_3Te_2 compositions of Kim and Chao (1991). This is a region where the Pd–Te–Bi ternary diagram is lacking in detail but an analysis (Table 2, anal. 6) can give a formula of $Pd_{8.88}(Te,Bi)_{4.12}$ which is close to telluropalladinite Pd_9Te_4. These tellurides are often associated with iridium and/or gold (Fig. 5*f,g*) and ten form single inclusions.

Group (iv): Pd–Te–Bi

The Pd–Te–Bi group contains 32–41 wt.% Pd, 25–37 wt.% Bi, 18–31 wt.% Te and 0 wt.% Sb. In the polished surface of nugget BW2-12 there are eight examples up to 4.5 μm across with high Bi content and no Sb; based on 13 analyses of examples 2 μm × 2 μm or larger that do not show evidence of interference from the Pt+Fe present in the host (Table 1). They usually occur as minor components within other Pd-PGM where they often form Bi-rich areas or internal bands with ill-defined margins that are readily distinguished by their lighter appearance on BSE images (Fig. 5*j*). The analyses of this group lie close the PdTe–PdBi solid-solution series and one analysis (Table 2, anal. 7) can be fitted to $Pd_3(Bi,Te)_2$. The synthetic phases Pd_9Te_4 and Pd_3Te_2 relate to the Pd–Te system and it is not clear if this is appropriate for phases containing 11–23 wt.% Bi. The analysis presented in Table 2 (anal. 8) is the average of 24 analyses and it lies further from the PdTe–PdBi series than others that have been reported (Cook *et al*., 2002) although it is not a good fit to a formula of Pd(Te,Bi). It actually fits $Pd_5(Te,Bi)_4$ rather well but such a phase has not been noted in experiments so a mix of Pd(Bi,Te) and $Pd_3(Bi,Te)_2$ may be a possible explanation. A part of one inclusion contains 6–7 wt.% Rh and more Te (33 wt.%) and may relate to the Rh–Te±(Pd–Bi) phase described below.

Group (v): Rh–Te±(Pd–Bi)

Phases with Rh–Te±(Pd–Bi) occur on the edges of Pd-tellurides from groups (iii) and (iv). They all show a darker appearance on BSE images and contain significant amounts of Rh. One of the three examples located is a Rh-, Te-rich phase containing 54–57 wt.% Te, 34–38 wt.% Rh, 1–3 wt.% Bi and 1–6 wt.% Pd. It is six–sided, measuring 1 μm × 3 μm and it occurs as a composite inclusion with Ir and Pd–Te–Sb. Platinum comprises 1–3 wt.% with no Fe; Pd and Ir are also low (1–5 wt.% Pd and 0–2 wt.% Ir) and Sb was not detected so interference from either the host or the other phases in the inclusion appears to be small so the six analyses appear to offer a reasonable indication of a composition close to RhTe despite the small grain size. The other two examples are Pd-rich phases with 6–16 wt.% Rh and more Te (33–38 wt.%) and appear to be related to the Rh–Te phase.

Iridium (Ir–Ru–Pt–Rh alloy)

Iridium is up to 4 μm across and occurs in 34 inclusions. It is found in association with Pd-tellurides and/or with Au and as small (2 μm) single crystals that contain more Ru and less Rh or Pt when not associated with the tellurides. Rarely iridium forms composite inclusions with laurite. More frequently iridium occurs at the edge of tellurides and extends into the host Pt_3Fe (Fig. 5*f,k*). Less often it is seen within the Pd-tellurides (Fig. 5*g*). The composition, based on 21 analyses of examples larger than 2 μm in each direction, is Ir 57–66, Ru 24–28, Pt 8–17 and Rh 0–3 wt.%.

Gold (Au–Pd–Cu alloy)

Gold between 0.1 and 7 μm long has been found in 21 inclusions. Many of them are irregular or subrounded (54%) with slightly diffuse boundaries but others show crystalline boundaries. They all have a very constant composition close to an average formula of $Au_{0.73}Pd_{0.18}Cu_{0.08}$, with very minor Pt or Fe. One example is shown in Table 2, anal. 9. Gold is commonly associated with Pd-tellurides and is often in contact with iridium (Fig. 5*e,f*). Occasionally it is associated with Pd-antimonides or it is in contact with osmium. The largest grain of Au found in this nugget (2.5 μm × 7 μm) is associated with an elongate (0.3 μm × 3 μm) crystal of cupriferous palladium ($Pd_{0.45}Pt_{0.28}Cu_{0.26}$) that extends from the Au to the core of the inclusion (Fig. 5*o*).

Gold almost always occurs at the edge of the inclusions, sometimes in elongate or L-shaped crystals, and more often in subhedral grains. Only three single inclusions of gold up to 4 μm across have been observed. Two of them are rounded whereas the other one shows six facets. Other Au

https://doi.org/10.1180/mgm.2018.85 Published online by Cambridge University Press

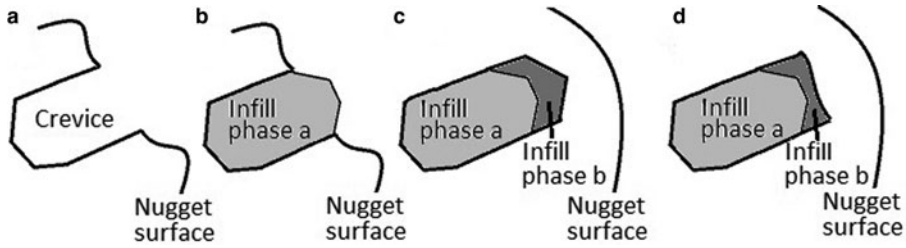

FIG. 6. Cartoon to illustrate the proposed formation of the inclusions.

inclusions with three facets enclose iridium (Fig. 5*p,q*). The composition, based on 13 analyses of examples larger than 2 μm in each direction, is Au 85–88, Pd 9–13 and Cu 2–4 wt.%.

Osmium (Os–Ir±Ru alloy)

Osmium has been located in five inclusions forming thin, lath-like crystals up to 2 μm long often occuring near the sides of the inclusions (Fig. 5*l,n*). The grains are too small for quantitative analyses but qualitative analyses suggest Os 37–58, Ir 30–42, Ru 0–9 and Pt 1–17 wt.%.

Discussion

The shape and genesis of the inclusions

The inclusion edges represent crystal faces controlled by the cubic host nugget and they formed as negative crystal voids. The inclusions subsequently filled the voids. This is the simplest and most consistent explanation for the evidence presented by this nugget. Many of the inclusions have straight edges on all sides but some have an irregular boundary on one side. The PGM attached to the outside of the nugget have a similar mineralogy to the inclusions. This suggests that the inclusions formed during growth of the nugget: the internal crystal faces of the voids represent crystal faces formed at the surface of the nugget during growth (Fig. 6*a*). The included minerals were formed in these crevices in the nugget surface (Fig. 6*b*). Continued growth closed the crevices so that the inclusions were either bounded entirely by crystal faces in the plane of the section (Fig. 6*c*) or by an irregular closure surface on one side (Fig. 6*d*). The external minerals are a continuation of this process. Many Pt_3Fe nuggets from the Freetown Peninsula contain between 1 and 5 PGM inclusions with the same features as those described here, so the conclusions from this nugget can be applied more generally.

The sequence of formation of the PGM

The textures can be judged using five criteria: (1) An inclusion with edges aligned to the structure of the host was once a void (Fig. 5*a*). (2) A zoned mineral in two parts separated by another phase where the two parts show the same zonation pattern indicates that the other phase has cut or replaced the zoned mineral. This is well illustrated by Fig. 5*a* where zoned laurite is cut by later irarsite–hollingworthite. (3) Laurite in association with irarsite–hollingworthite where one or both of those minerals are zoned is an indication of varying PGE+As+S supply leading to the formation of laurite followed by irarsite–hollingworthite with a return to laurite. This is illustrated by Fig. 5*b, c* where irarsite replaces zoned laurite and by Fig. 5*d* where zoned irarsite surrounds zoned laurite. (4) A mineral attached to the wall of a void grew first and the mineral filling the remainder of the void was later. For example, Fig. 5*e* shows laurite attached to the wall of the inclusion surrounded by later Pd–Te–Sb. (5) A rounded or diffuse phase surrounded by another phase is later than its host as in Fig. 5*j,p,q*.

These criteria lead to the following tentative order of formation: isoferroplatinum host → laurite-irarsite–hollingworthite-laurite → gold → Pd–Au, Pd–Pt–Cu alloys → Pd–Sb–Te → Pd–Te–Sb–Bi → Pd–Te–Bi–Sb → Rh–Te±(Pd–Bi) → iridium → osmium, as set out in Table 3.

Among the Pd–Te–Bi–Sb phases there is a progressive increase in the Bi-content at the expense of Sb.

Genesis of the inclusions

If the inclusions had been trapped during growth of the nugget in a magmatic environment the

https://doi.org/10.1180/mgm.2018.85 Published online by Cambridge University Press

TABLE 3. Order in which the minerals in the inclusions appear to have been formed.

	Order of formation	Texture which indicates the order of formation	Examples in Fig. 5.
Early	Isoferroplatinum	Host containing voids shaped by internal facets of the host. These voids filled by the minerals listed below.	*a–q* especially *a,b,c,d, m,n,o*
	Laurite–irarsite –hollingworthite–laurite	Zoned irasite–hollingworthite cut by later laurite	*a,b*
		Zoned laurite cut by later irasite–hollingworthite	*c*
		Zoned irasite–hollingworthite surrounding zoned laurite	*d*
	Gold	Gold in facetted void containing later iridium	*p,q*
	Pd–Au–alloys	Pd–Au alloy surrounded by later Pd–Sb–Te	not shown
	Pd–Pt–Cu alloy	Pd–Pt–Cu formed after gold and surrounded by even later Pd–Sb–Te	*o*
	Pd–Sb–Te	Pd–Sb–Te containing later osmium	*n*
	Pd–Te–Sb–Bi	Laurite and gold surrounded by later Pd–Te–Sb–Bi	*e*
		Pd–Te–Sb–Bi containing later iridium	*k* (upper inclusion)
	Pd–Te–Bi–Sb	Pd–Te–Sb–Bi containing later, more Bi–rich, Pd–Te–Bi–Sb	*i,j*
		Pd–Te–Sb–Bi containing later Pd–Te–Bi–Sb, both cut by later osmium	*l*
		Pd–Te–Bi–Sb after Au and containing later iridium	*f*
	Pd–Te–Bi	Pd–Te–Sb–Bi containing later Pd–Te–Bi	*k* (lower inclusion)
	Rh–Te±(Pd–Bi)	Occurs as later inclusions in Pd–Te–Sb–Bi and Pd–Te–Bi–Sb	not shown
	Iridium	Iridium occurs as a later inclusion within gold	*p,q*
Late		Iridium formed later than Pd–Te–Bi–Sb and gold	*f*
		Iridium formed later than Pd–Te–Bi–Sb	*g*
	Osmium	Osmium formed later than Pd–Sb–Te	*n*
		Osmium formed later than Pd–Te–Sb–Bi and Pd–Te–Bi–Sb	*l*

inclusions would have random orientations. In addition, it is possible to envisage a few inclusions being trapped in this way but more difficult to see a situation in which so many PGM were gathered together in a small volume ready to be encompassed by a growing nugget. Isoferroplatinum does not normally have a cleavage and the inclusions do not lie along some cleavage plane or another weakness in the host. Exsolution of the PGE from the isoferroplatinum host would not form inclusions with the observed shapes. The external attached minerals, laurite, irarsite and cuprorhodsite, are not identical to those in the inclusions but are considered to be an evolved part of the process that formed the inclusions.

The presence of these inclusions is not unique to the nugget BW2 and the same features can be seen (albeit less abundantly) in other nuggets from the area. One argument against a neoform origin for these nuggets was that the inclusions could be considered to be either primary minerals or sulfide droplets caught up in a magmatic nugget or, in the case of thin Os-rich lamellae, to be exsolution products (Hattori *et al.*, 1991). While these processes undoubtedly occur, the inclusions examined here formed later than their host as shown by the measurements presented in Fig. 3. They are not earlier phases entrapped by the host and they do not exhibit the texture of exsolution lamallae. The arguments for a neoform origin of nuggets found in the rivers draining the Freetown intrusion have been put forward and in summary they are that there is a distinctive difference between the PGM assemblage in the fresh rocks and the alluvium. Cooperite, abundant in the fresh rocks, is less abundant in the streams whereas Pt–Fe alloys form a much larger proportion of the alluvial mineral suite. Hongshiite appears as an alteration to the alluvial Pt–Fe alloys and tulameenite is more abundant. Palladium minerals in the fresh rocks are not encountered in the alluvium. Oxidized PGM in the weathered rocks are a transitional stage in the alteration of the primary PGM and the formation of the placer nuggets. Their fragile textures indicate that they are the result of alteration of primary PGM and mobility of PGE. The Pt–Fe alloys in the weathered rocks show an almost continuous range of composition from Pt_3Fe to PtFe and nearly to $PtFe_3$, indicating varying degrees of disordering due to low-temperature alteration. There is a significant loss of Pd relative to Pt. Pt/Pd ratios below 75 in the host rocks rise to 100–500 in the

https://doi.org/10.1180/mgm.2018.85 Published online by Cambridge University Press

alluvial deposits demonstrating the greater mobility of Pd in solution. Some Pt–Fe alloys in the placers contain a small proportion of Cu (0.3–2.7 wt.%) that increases the compositional variability and degree of disorder. Alluvial tulameenite, hongshiite and native Cu are present and appear to be a part of the process with some Pt–Fe nuggets being replaced by hongshiite at the edges. Apart from the presence of smaller grains of tulameenite, these features are not encountered in the fresh rocks. There is a three-orders of magnitude difference in size between the PGM seen in the fresh rocks compared with the larger alluvial mineral suite. The delicate and well-preserved crystal features of some nuggets suggest a local origin; damaged nuggets have had a longer residence time in the rivers. These are not delicate PGM protected until recently by enclosing silicates. Some alluvial PGM occur in drainage for which there is no known source for a derivation by mechanical erosion (Bowles *et al*., 2013, 2017, 2018). A coating of organic material on the nuggets is evidence of an association between the nuggets and organic material and may indicate involvement of organic material or bacterial action during formation of the nuggets demonstrated by Reith *et al*. (2016) and Campbell *et al*. (2018).

There is a relevant comparison with the abundant Pt, Pd, and gold phases from the Bon Accord Ni-oxide body (Barberton greenstone belt, South Africa) which occur as minute inclusions (<3 μm) in trevorite ($NiFeO_4$) and larger (5–70 μm) free aggregates. These inclusions consist of Pd–Sb, Pd–Sb–As, Pd–Cu–Sb, Pt–Sb, Pt–As–S, Ru–As–S, Ru–S phases and free grains of Ni–Fe–As. The free aggregates consist of sperrylite ($PtAs_2$), members of the sobolevskite–kotulskite series and electrum. The paragenetic relationships indicate that the PGM and electrum are of secondary origin (Zaccarini *et al*., 2014). The presence of $(Pd,Pt)_{20}(Te,Sb,Bi)_7$ in the nugget examined here can be compared with the keithconnite inclusion within Pt_3Fe described previously from the Freetown alluvial suite (Bowles, 2000*b*). It is also relevant to make comparisons with the occurrence of vincentite $(Pd,Pt)_3(Sb,Te,As)$ described by Stumpfl and Tarkian (1974) and Tarkian *et al*. (2002) which was found as small (7–10 μm, rarely up to 40 μm) inclusions with an osmium inclusion in nuggets of alluvial Pt–Fe alloy from the Riam Kanan River, Borneo. A similar phase $(Pd,Pt)_3(Te,As)$ was recorded by Augé and Legendre (1992) in alluvial Pt–Fe nuggets from eastern Madagascar together with osmium alloy, laurite, erlichmanite, cooperite, braggite, kashinite, hollingworthite, keithconnite and iridium oxide. Arsenic formed a constituent in the latter occurrences and the As content found in the inclusions described here is limited to 0–1 wt.% in a few of the Sb-rich inclusions from groups (i) and (ii). The hydrothermal copper ores of the New Rambler Mine, Wyoming (McCallum *et al*., 1976) contain rhodian sperrylite, merenskyite, kotulskite, michenerite and $PdTe_2$ ('phase C'). Three other tellurides are present; 'phase A' $(Pd)_5(Bi,Sb)_2$, 'phase B' $Pd_5(Te,Bi,Sb)_2$ and 'phase D' Pd–Bi–Te, which were considered to be supergene or associated with supergene alteration.

It is clear that neoform nuggets are present and this raises many questions concerning how they are formed. Bowles (1986) suggested a purely chemical origin based on suitable Eh and pH conditions and the high rainfall in the area. The contribution of organic compounds is relevant and it has been shown that humic and fulvic acids present in the soils are capable of taking the PGE into solution from the metals and PGM (Bowles *et al*., 1995). Recent developments in biogeochemistry have shown (Reith *et al*., 2016; Campbell *et al*., 2018) that bacteria are capable of forming PGM from solution so possible steps in the neoforming process are becoming clear. The evidence presented here contributes a further control on the neoforming process with a requirement for a varying transport of metals in solution or the growth process to pass through differing stages that permit the formation of the host nuggets and the sequence of minerals seen in the inclusions.

Conclusions

The inclusions, with faces parallel to the crystal faces of the host, show that the inclusions represent voids formed during growth of the nugget. These voids were filled by PGM and gold alloys during nugget growth and that process continued with the formation of PGM on the present surface of the nugget. The continuity of the orientation of the inclusions across the host isoferroplatinum shows that the host is a single crystal, not an agglutination of smaller crystals. The zoned laurite and irarsite–hollingworthite are clearly crystalline on the scale of the inclusions whilst some of the Pd–Te–Sb–Bi inclusions, especially those containing diffuse area of varying composition, may be cryptocrystalline aggregates.

The inclusions contain laurite, irarsite–hollingworthite, Pd-Cu-bearing gold, Sb-rich

https://doi.org/10.1180/mgm.2018.85 Published online by Cambridge University Press

keithconnite ($Pd_{19.98}(Te,Sb,Pt,Bi)_{7.03}$), keithconnite ($(Pd,Pt)_{20.06}(Te,Sb,Bi)_{6.94}$), telluropalladinite ($Pd_{8.88}(Te,Bi)_{4.12}$), '$Pd_5(Te,Bi)_4$', RhTe, Ir-alloy and Os-alloy. In some instances the laurite is zoned, in other cases the irarsite–hollingworthite is zoned and the laurite sometimes contains some As. The textural evidence shows examples of laurite replacing irarsite–hollingworthite and vice versa. The zonation, the mutual replacement and the As content of the laurite indicate that these minerals were formed in association under conditions of varying PGE+As+S supply. Formation of the arsenic- and sulfur-bearing minerals was succeeded by gold, Pd–Au alloy and Pd–Pt–Cu alloy. The Pd–Te–Sb–Bi minerals were formed subsequently, probably in the sequence Pd-Cu-bearing gold, $Pd_{19.98}(Te,Sb,Pt,Bi)_{7.03}$, $(Pd,Pt)_{20.06}(Te,Sb,Bi)_{6.94}$, $Pd_{8.88}(Te,Bi)_{4.12}$, '$Pd_5(Te,Bi)_4$', RhTe, Ir-alloy and Os-alloy. This sequence follows a course of decreasing Bi and increasing Sb and Rh. The two $Pd_{19.98}(Te,Sb,Pt,Bi)_{7.03}$, $(Pd,Pt)_{20.06}(Te,Sb,Bi)_{6.94}$ groups may be Sb-rich varieties of keithconnite. $Pd_5(Te,Bi)_4$ has not been reported during experiments, it is close to the kotulskite–sobolevskite solid-solution series (Pd(Bi,Te)) and may be a mix of Pd(Bi,Te) and $Pd_3(Bi,Te)_2$.

The list of differences between the PGM of the layered gabbros and the alluvial suite encompasses the mineral assemblage, transitional oxidized PGM and disordered Pt–Fe alloys, loss of Pd, Cu modification of the Pt–Fe alloys, the three-orders of magnitude difference in size, alluvial crystals that are delicate in structure or external finish, an organic coating to alluvial PGM, and the presence of alluvial PGM in a drainage basin with no apparent source for mechanical derivation. This list can now be extended by the addition of oriented PGM+Au alloys and tellurides that have occupied voids in the neoform nuggets. Similar inclusions have not been observed in the Pt–Fe alloys present in the rocks of the Freetown Intrusion.

Acknowledgements

This work has been made possible by the technical support of Drs. J. Rodríguez, R.S. García, M. Sánchez-Lorda (SGIker, UPV/EHU) and generous funding for SS from the Department of Education, Universities and Research of the Basque Government (Refs. BFI-2011-254, IT762-13). Panning to recover the nuggets was done by the people of York, Sierra Leone who we thank for their cheerful efforts. This work formed part of a Post-doctoral appointment for Saioa Suárez at Cardiff under the supervision of Prof. H.M Prichard and JFWB. Hazel contributed to this study, to discussion of the ideas and to writing the first version of the manuscript. She was excited by the evidence presented here and discussed the content of this paper at length with the other authors. This paper has greatly benefitted from constructive advice provided by Iain McDonald, Brian O'Driscoll and two anonymous reviewers.

References

Augé, T. and Legendre, O. (1992) Pt-Fe Nuggets from alluvial deposits in eastern Madagascar. *The Canadian Mineralogist*, **30**, 983–1004.

Bowles, J.F.W. (1986) The development of platinum-group minerals in laterites. *Economic Geology*, **81**, 1278–1285.

Bowles, J.F.W. (2000*a*) A primary platinum occurrence in the Freetown Layered Intrusions, Sierra Leone. *Mineralium Deposita*, **35**, 583–586.

Bowles, J.F.W. (2000*b*) Prassoite, vysotskite and keithconnite from the Freetown Layered Complex, Sierra Leone. *Mineralogy and Petrology*, **68**, 75–84.

Bowles, J.F.W., Giże, A.P., Vaughan, D.J., Norris, S.J. (1995) Organic controls on platinum-group element (PGE) solubility in soils: initial data. *Chronique de la Recherche Minière*, **520**, 65–73.

Bowles, J.F.W., Prichard, H.M., Suárez, S. and Fisher, P.C. (2013) The first report of platinum-group minerals in magnetite-bearing gabbro, Freetown Layered Complex, Sierra Leone: occurrences and genesis. *The Canadian Mineralogist*, **51**, 455–473.

Bowles, J.F.W., Suárez, S., Prichard, H.M. and Fisher, P.C. (2017) Weathering of PGE-sulfides and Pt-Fe alloys, in the Freetown Layered Complex, Sierra Leone. *Mineralium Deposita*, **52**, 1127–1144.

Bowles, J.F.W., Suárez, S., Prichard, H.M. and Fisher, P.C. (2018) The mineralogy, geochemistry and genesis of the alluvial platinum-group minerals of the Freetown Layered Complex, Sierra Leone. *Mineralogical Magazine*, **82**(S1), S223–S246.

Campbell, G., MacLean, L., Reith, F., Brewe, D., Gordon, R.A. and Southam, G. (2018) Immobilisation of platinum by *Cupriavidus metallidurans*. *Minerals*, **8**, 10, 1–18.

Cook, N.J., Ciobanu, C.L., Merkle, R.K.W. and Bernhardt, H.-J. (2002) Sobolevskite, Taimyrite, and Pt_2CuFe (Tulameenite?) in complex massive Talnakhite Ore, Noril'sk Orefield, Russia. *The Canadian Mineralogist*, **40**, 329–340.

Hattori, K.H., Cabri, L.J. and Hart, S.R. (1991) Osmium isotope ratios of PGM grains associated with the Freetown Layered Complex, Sierra Leone, and their origin. *Contributions to Mineralogy and Petrology*, **109**, 10–18.

https://doi.org/10.1180/mgm.2018.85 Published online by Cambridge University Press

Kim, W.-S. and Chao, G.Y. (1991) Phase relations in the system Pd-Sb-Te. *Canadian Mineralogist*, **29**, 401–409.

McCallum, M.E., Loucks, R.R., Carlson, R.R., Cooley, E. F. and Doerge, T.A. (1976) Platinum metals associated with hydrothermal copper ores of the New Rambler Mine, Medicine Bow Mountains, Wyoming. *Economic Geology*, **71**, 1429–1450.

Pollett, J.D. (1931) Platinum mining in Sierra Leone. *Engineering and Mining World*, **2**, 747–748.

Pollett, J.D. (1951) The geology and mineral resources of Sierra Leone. *Colonial Geology and Mineral Resources*, **2**, 3–28.

Reith, F., Zammit, C.M., Shar, S.S., Etschmann, B., Bottrill, R., Southam, G., Ta, C., Kilburn, M., Oberthür, T., Bail, A.S. and Brugger, J (2016) Biological role in the transformation of platinum-group mineral grains. *Nature Geoscience*, **9**, 294–298.

Stumpfl, E.F. and Tarkian, M. (1974) Vincentite, a new palladium mineral from south-east Borneo. *Mineralogical Magazine*, **39**, 525–527.

Tarkian, M., Klaska, K.-H. and Stumpfl, E.F. (2002) New data on vincentite. *The Canadian Mineralogist*, **40**, 457–461.

Zaccarini, F., Tredoux, M., Miller, D.E., Garuti, G., Aiglsperger, T. and Proenza, J.A. (2014) The occurrence of platinum-group element and gold minerals in the Bon Accord Ni-oxide body, South Africa. *American Mineralogist*, **99**, 1774–1782.

https://doi.org/10.1180/mgm.2018.85 Published online by Cambridge University Press